

## Evaluation of Material Degradation of 1Cr-1Mo-0.25V steel using Ball Indentation Method

**Chang-Sung Seok\***

*School of Mechanical Engineering, Sungkyunkwan University, 300 Chunchun-dong, Jangan-gu, Suwon, Kyonggi-do, 440-746, Korea*

**Jeong-Pyo Kim**

*Digital Module Division, Sound Solution Team(R & D), SamSung Electro-Mechanics Co., LTD., 314 Maetan 3-Dong, Yeongtong-Gu, Suwon, Kyunggi-Do, 442-743, Korea*

**Jae-Mean Koo**

*School of Mechanical Engineering, Sungkyunkwan University, 300 Chunchun-dong, Jangan-gu, Suwon, Kyonggi-do, 440-746, Korea*

The BI (Ball Indentation) method has the potential to assess the mechanical properties and to replace conventional fracture tests. In this study, the effect of aging on mechanical behavior of 1Cr-1Mo-0.25V steels procured by isothermal aging heat-treatment at four different aging times in the range of 0~1820 hours at 630°C, were investigated using BI system.

**Key Words :** Material Properties, Ball Indentation, Degradation, Fracture Toughness, 1Cr-1Mo-0.25V

### Nomenclature

$\sigma_t$	: True stress
$\varepsilon_p$	: True plastic strain
$K$	: Strength coefficient
$D$	: Diameter of ball indenter
$d_p$	: Plastic indentation diameter
$d_t$	: Total indentation diameter
$E_1$	: Elastic modulus of indenter
$E_2$	: Elastic modulus of specimen
$h_t$	: Total depth of indentation
$K_{IC}$	: Fracture toughness
$K_Q$	: Fracture toughness (not satisfying the size requirements)
$P_{max}$	: Maximum indentation load
$S$	: Inclination of indentation load-depth curve
$Q$	: Activation energy
$R$	: Gas constant

### 1. Introduction

Low-alloy ferrite steel, 1Cr-1Mo-0.25V, is widely used as a material for high temperature structural components in electric power generation industries because of optimum combination of its good mechanical properties and relatively low cost. However, as it has the problem that its mechanical properties are degraded easily in long-term service at high temperatures, it is necessary to estimate the degree of degradation exactly in order to assure the safety in service. The destructive method is reliable to the evaluation of material degradation, but there is a difficulty in extracting specimens from industrial facilities in service. Therefore the evaluation of material degradation by the nondestructive methods such as ultrasonic tests, electric resistance tests (Nham and Kim, 1998 ; Seok, et al., 2000) and replica tests is required. One of such non-destructive methods is a ball indentation technique (Haggag and Nannstad, 1989 ; Haggag, 1993).

In this study, the effect of aging on the me-

\* Corresponding Author,  
**E-mail :** Seok@skku.edu  
**TEL :** +82-31-290-7446; **FAX :** +82-31-290-7482  
School of Mechanical Engineering, Sungkyunkwan University, 300 Chunchun-dong, Jangan-gu, Suwon, Kyonggi-do, 440-746, Korea (Manuscript Received December 16, 2003; Revised July 1, 2004)

chanical properties of 1Cr-1Mo-0.25V steel has been investigated using the BI technique and compared with the properties from the conventional tensile test and the fracture toughness test. Four different class materials obtained by isothermal aging heat-treatment for 0, 453, 933, 1820 hours at 630°C, were tested.

## 2. Ball Indentation Technique

### 2.1 Ball indentation system

The BI system was developed to determine mechanical properties of material as a non-destructive method. The BI system is based on an automated ball indentation (ABI) technique and involves strain-controlled multiple indentations at a single penetration location on a polished surface by a small spherical indenter. The indentation loads and penetration depths are measured during the test, and are used to calculate the stress-strain values from elasticity and plasticity theories and semi-empirical relationships which govern the behavior of material under multiaxial indentation loading. By analyzing the stress-strain curve, tensile parameters of material such as yield strength, tensile strength, strength coefficient and strain hardening exponent can be evaluated (Haggag and Murty, 1997).

As seen in Fig. 1, BI system is composed of the hardware part including load cell, LVDT, indenter, etc. and the software part which calculates material properties from electric signals transferred by the A/D converter. The test is fully automated with a PC and a test controller to control

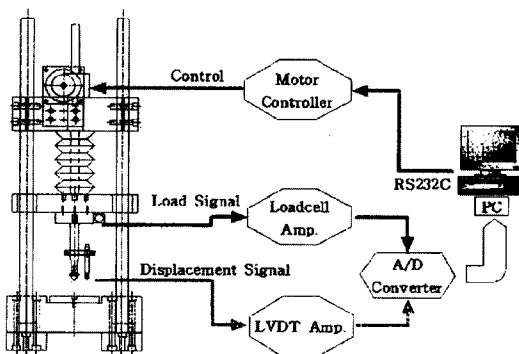


Fig. 1 Schematic diagram of the BI system

the test and analyze the data including real-time graphics, digital display of load-depth test data, etc.. The indenter is moved into the material at a constant speed and the indentation depth is gradually increased to a maximum limit with partial unloading. The loading-unloading process is carried out in several steps. Indentation load and penetration depth are monitored by using an on-line load cell and a linear variable differential transducer with a high resolution, respectively. Thus material properties can be obtained from indentation load-depth curve.

### 2.2 Theory of indentation

Tabor (1951) was the first to correlate indentation hardness and strain associated with a spherical indenter to uniaxial tensile test results. These correlations are based on three premises: (i) monotonic true stress-true plastic strain curves obtained from tension and compression testing are reasonably similar; (ii) indentation strain correlates with true plastic strain in a uniaxial tensile test; and (iii) mean ball indentation pressure correlates with true flow stress in uniaxial tensile test. These three premises are well established for several materials (Haggag, 1993). It should be noted that, with respect to the first premise, the engineering stress-strain curves show correlation only up to ultimate tensile stress since there is no necking instability in compressive loading. Thus, although the principle of ball indentation to study deformation behavior of materials is not new, BI technology has several distinctly unique features. The BI technique of loading followed by partial unloading during indentation enables indentation depth  $h_p$  associated with plastic deformation to be properly estimated.

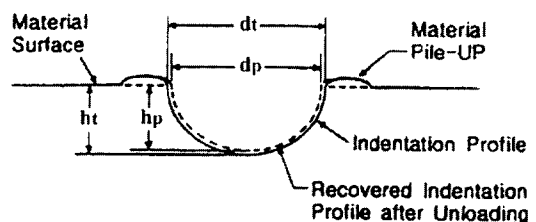


Fig. 2 Schematic diagram of an ball indentation profile

The plastic diameter can then be determined from  $h_p$  even if the sinking-in and piling-up of the test material around the indentation are not known. Fig. 2 is a schematic representation of the indentation profile in a BI test.

### 2.2.1 Stress-strain relation

The true stress versus true strain curve can be represented by the power law equation.

$$\sigma_t = K \varepsilon_p^n \quad (1)$$

where  $\sigma$  is the true stress and  $\varepsilon_p$  is the true plastic strain.  $n$  is the strain hardening exponent and  $K$  is the strength coefficient (provided the plot of the data  $\ln \sigma$  versus  $\ln \varepsilon_p$  is linear). Values of  $K$  and  $n$  are determined by linear regression analysis of the data. For  $\varepsilon_p = n$  (Mathew and Murty, 1999), Eq. (1) will provide the expression for true ultimate tensile strength. The engineering value of ultimate tensile strength can be obtained from the following equation.

$$S_{UTS} = K \left( \frac{n}{e} \right)^n \quad e = 2.71 \quad (2)$$

True plastic strain  $\varepsilon_p$  can be obtained from the following equation.

$$\varepsilon_p = 0.2 d_p / D \quad (3)$$

$D$  is the diameter of the ball indenter and  $d_p$  is plastic indentation diameter.  $d_p$  can be expressed as follows.

$$d_p = \sqrt[3]{\frac{0.5CD[h_p^3 + (d_p/2)^2]}{[h_p^2 + (d_p/2)^2 - h_p D]}} \quad (4)$$

where  $C = 5.47P(1/E_1 + 1/E_2)$ .  $E_1$  and  $E_2$  are the elastic moduli of indenter and specimen, and true plastic stress  $\sigma_t$  can be calculated from the following equation.

$$\sigma_t = 4P / \pi d_p^2 \delta \quad (5)$$

where

$$\sigma = \begin{cases} 1.12 & \phi \leq 1 \\ 1.12 + \tau/n\phi & 1 < \phi \leq 27 \\ 2.87\alpha_m & \phi > 27 \end{cases}$$

$$\phi = \frac{\varepsilon_p E_2}{0.43\sigma_t}$$

$$\tau = (2.87\alpha_m - 1.12)$$

The parameter  $\phi$  represents the three stages of

plastic zone development under the indenter; (i) nucleation of plastic zone ( $\phi \leq 1$ ), (ii) transition to the development of plastic zone ( $1 < \phi \leq 27$ ), and (iii) fully developed plastic zone ( $\phi > 27$ ). The parameter  $\phi$  depends on the flow stress and plastic strain, and its value is calculated by iteration. The parameter  $\alpha_m$  depends mainly on the strain rate sensitivity and work-hardening characteristics of the material;  $\alpha_m$  varies from 0.9 to 1.25 for different materials, typically with a value of 1.0 for low strain rate sensitive materials. In this study  $\alpha_m$  of 1Cr-1Mo-0.25V steel was obtained from comparing true stress-true strain curve by a tensile test with one by a BI test.

### 2.2.2 Yield Stress

The flow stress corresponding to the initiation of plastic deformation ( $\phi = 1$ ) is not determined from Eq. (5) because the corresponding strains are too small to be directly measured during the indentation test. Therefore, a different approach is used for the estimation of the yield strength. Yield strength is estimated from the relationship between the mean pressure and impression diameter as developed by Meyer. Data points from all loading cycles (maximum value of  $d_t/D = 1.0$ ) are fit by linear regression analysis to the following relationship:

$$\frac{P}{d_t^2} = A \left( \frac{d_t}{D} \right)^{m-2} \quad (6)$$

$d_t$  is the total diameter of the impression and  $m$  is the Meyer's exponent ( $m$  generally has a value between 2 and 2.5) and  $A$  is a material yield parameter obtained from the regression analysis. The value of  $d_t$  is determined from total depth of penetration (Fig. 2) using the following equation.

$$d_t = 2\sqrt{Dh_t - h_t^2} \quad (7)$$

where  $h_t$  is the total depth of the indentation. The yield strength ( $\sigma_y$ ) is proportional to the Meyer hardness ( $4P/\pi d^2$ ).  $d$  is the final impression diameter and can be calculated using the following equation.

$$\sigma_y = \beta_m A \quad (8)$$

Here  $\beta_m$  and  $A$  are constants for a given materials. The value of  $\beta_m$  is determined from yield

strength obtained from standard tensile tests, and the value of  $A$  is obtained from BI tests.

**2.2.3 Brinell hardness**

The Brinell hardness, HB, can be determined using the following equation.

$$HB = \frac{2P_{max}}{[\pi D(D - (D^2 - D_f^2)^{0.5})]} \quad (9)$$

where  $P_{max}$  is the maximum indentation load and  $D_f$  is the final diameter of the indentation circle. The ultimate tensile strength can also be estimated from the Brinell hardness.

**2.2.4 Indentation Energy to Fracture (IEF)**

IEF proposed by Haggag, et al. (1990) in order to calculate the fracture toughness by using on BI tester, and it is defined as absorbed indentation energy to cleavage fracture of material in BI test. It can be expressed as follows.

$$IEF = \frac{S}{\pi} \ln\left(\frac{D}{D - h_f}\right) \quad (10)$$

where  $S$  is the inclination of indentation load-depth curve and  $h_f$  is the depth of virtual fracture when the maximum normal stress reaches the critical stress of cleavage fracture. To calculate the depth of the virtual fracture, fracture stress was obtained from a tensile test. The virtual stress of indentation fracture corresponding to this fracture stress was defined as the representative fracture stress. Then the depth of indentation fracture for the representative fracture stress is the depth of the virtual fracture.

**3. Experimental Procedure**

**3.1 Degradation material**

The present investigation has been carried out

using the four classes of the thermally aged 1Cr-Mo-0.25V steel specimen prepared by artificially accelerated aging method. Degradation time was determined from the self diffusion theory of Fe by eq. (11) and Eq. (12).  $D_1$  and  $D_2$  of the equations are diffusion coefficients for each 538°C and 630°C and the degradation time ( $t_2$ ) for 630°C is followed as Eq. (13) (Abdel-Latif, et al., 1982).

$$D_1 = D_0 \exp\left[-\frac{Q}{RT_1}\right] = \frac{C}{t_1} \quad (11)$$

$$D_2 = D_0 \exp\left[-\frac{Q}{RT_2}\right] = \frac{C}{t_2} \quad (12)$$

$$t_2 = t_1 \exp\left[-\frac{Q}{R}\left(\frac{1}{T_2} - \frac{1}{T_1}\right)\right] \quad (13)$$

where  $R$  is the gas constant (8.314 J/kmol/K) and  $Q$  is the activation energy (65 kcal/mol) for the self diffusion of Fe and  $T_1, T_2$  are degradation temperature and  $t_1, t_2$  are degradation time. Aging was carried out for four different aging times, 0, 453, 933, 1820 hours at 630°C each. The chemical composition of the specimen and the aging time at 630°C for equivalent microstructure served at 538°C are given in Table 1 and Table 2 respectively.

**3.2 Experiments**

Ball indentation tests were performed on materials degraded at the laboratory. A tungsten carbide spherical indenter of 0.508 mm diameter was used for the BI tests. The tests were carried out with an indenter velocity of 0.005 mm/s at room temperature. The loading-unloading process was carried out in seven steps. Values of BI parameters  $\alpha_m$  and  $\beta_m$  were derived by equating yield and tensile strengths from standard tensile tests with the BI tests of virgin material at room temperature.

**Table 1** Chemical compositions of 1Cr-1Mo-0.25V steel

Element	C	Si	Mn	S	P	Ni	Cr	Mo	V	Sn
Composition (wt. %)	0.29	0.01	0.74	0.004	0.007	0.60	1.29	1.24	0.25	0.0047

**Table 2** Determination of aging time at 630°C for equivalent microstructure serviced at 538°C

Time in Serve at 538°C (hour)	0	25,000	50,000	100,000
Equivalent Time at 630°C (hour)	0	453	933	1,820

According to ASTM E 8, tensile tests were performed with standard tensile specimens at room temperature. The fracture toughness ( $K_{IC}$ ) test was carried out using a 25 ton hydraulic dynamic tester according to ASTM E 399. CT typed specimens, 25.4mm thick, were used. But because the tests didn't satisfy the size requirements for a valid  $K_{IC}$ , the results of toughness tests were transcribed as  $K_Q$ .

Hardness tests were conducted using Vickers hardness tester. The surface of the specimen was polished mechanically using  $Al_2O_3$  powders and the test load was 9.8N. After tests, the values of Vickers hardness were converted into those of Brinell hardness as to ASTM E 140 in order to be compared with the values from BI tests.

### 4. Results and Discussion

#### 4.1 Microstructure

Microstructures of the degradation materials have been observed using an optical microscope. Fig. 3 shows the microstructures of the material for each degradation time, which shows a slight increase of carbide to cause degradation. Especially the microstructure of 1820 hour of aged material shows precipitation along the grain boundaries as compared to the others. Because de-

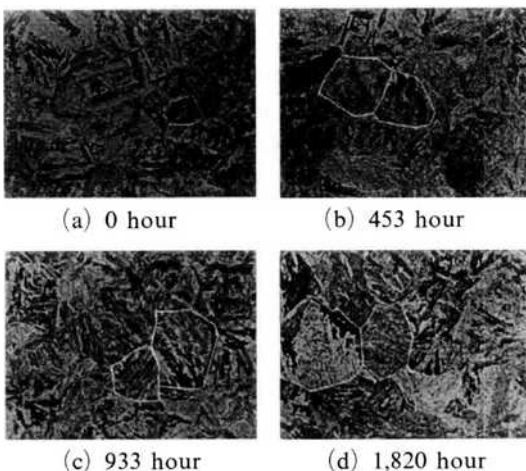


Fig. 3 Microstructure for each material after aging for with magnification of 400 (a) 0 hour (b) 453 hour (c) 933 hour and (d) 1,820 hour at 630°C

crease in strength by aging is directly attributed to coarsening of carbides and increasing of precipitates along the boundaries, the changes of microstructure with increase of aging time are expected to decrease in strength.

#### 4.2 Tensile and hardness behavior

Values of  $a_m=1.25$  and  $\beta_m=0.225$  were thus estimated using yield stress of 711MPa and ultimate tensile stress of 844MPa by standard tensile tests. These values of  $\alpha$  and  $\beta$  were used in the analysis of all BI data.

Fig. 4(a) and Fig. 4(b) show the comparison

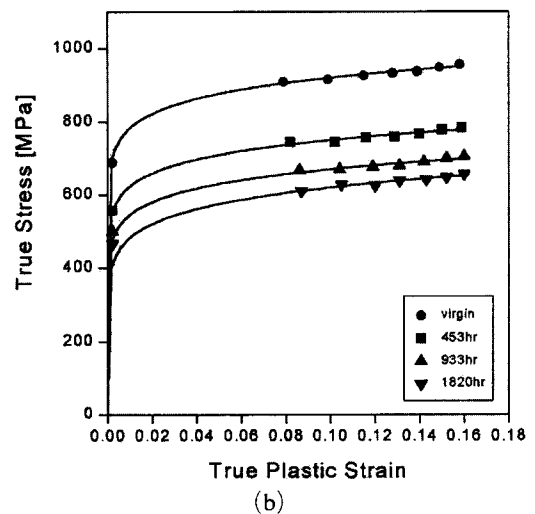
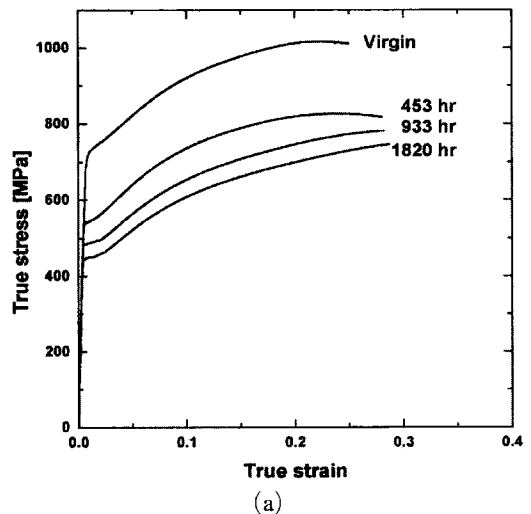


Fig. 4 True stress-true strain curves by (a) the tensile test and (b) the BI test

**Table 3-1** Results of BI tests

Degraded Time [hour]	Brinell Hardness [HB]					Yield Strength [MPa]					Tensile Strength [MPa]				
	1	2	3	Mean	Dev.	1	2	3	Mean	Dev.	1	2	3	Mean	Dev.
0	287	291	289	289	2.83	687	702	690	693	11	830	841	837	836	7.83
453	241	230	234	235	7.83	538	561	558	552	17.1	690	678	681	683	8.68
933	213	202	209	208	7.83	489	504	500	498	10.8	600	610	607	606	7.18
1,820	185	199	194	193	9.97	186	195	194	192	6.71	572	558	562	564	10.1

**Table 3-2** Results of BI tests

Degraded Time [hour]	Strain Hardening Exponent					Strength Coefficient [MPa]					IEF [mJ/mm <sup>2</sup> ]
	1	2	3	Mean	Dev.	1	2	3	Mean	Dev.	
0	0.05	0.045	0.07	0.06	0.01	1002	1125	1019	1049	91.1	560
453	0.075	0.089	0.08	0.08	0.01	924	860	903	895.7	45.7	460
933	0.1	0.09	0.09	0.09	0.01	800	854	823	825.7	38.3	415
1,820	0.15	0.13	0.11	0.13	0.02	753	820	798	790.3	47.9	386

**Table 4** Results of tensile tests, fracture toughness tests

Degraded Time [hour]	Yield Strength (0.2% offset) [MPa]	Tensile Strength [MPa]	$K_Q$ [Nmm <sup>-3/2</sup> ]
0	711	844	3,863
453	533	676	3,304
933	481	615	2,761
1,820	450	582	1,771

of the stress-strain curves from BI test and tensile tests for virgin and aged materials respectively. The results of BI tests and tensile tests are summarized in Table 3 and Table 4 respectively.

Figure 5 shows the effect of normalized factors, i.e., Brinell hardness, tensile strength of BI tests, indentation energy to fracture (IEF) and tensile strength of tensile tests on degraded time at in-service temperature, 538°C. Normalized factors divide the values of aged materials by those of virgin. This result shows that normalized Brinell hardness agrees well with others. Hence, it is seen that the effect of those on degraded time can be estimated by Brinell hardness.

Figure 6 shows the effect of the others, i.e., strain hardening exponent, strength coefficient and fracture toughness on degraded time at in-service temperature, 538°C. Brinell hardness and strength coefficient are not linearly related, but strain hardening exponent and fracture toughness are

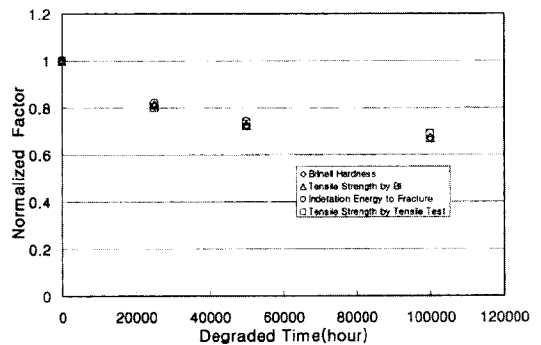


**Fig. 5** Effect of normalized factor on degraded time at service temperature

linearly related with degraded time. That is,

$$\frac{n}{n_0} = A_{at} + 1 \tag{14}$$

$$\frac{K_Q}{K_{Q0}} = B_{at} + 1 \tag{15}$$

where  $t$  is the degraded time and  $n_0$  and  $K_{Q0}$  are

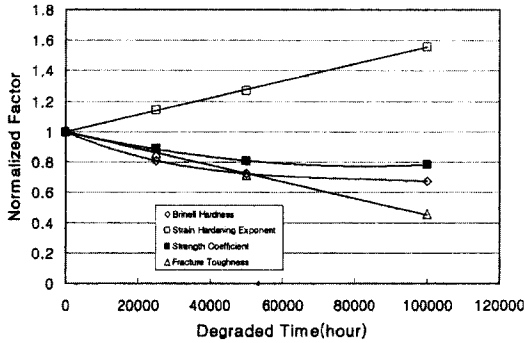


Fig. 6 Effect of normalized factor on equivalent degraded time at service temperature

strain hardening exponent and fracture toughness of virgin material respectively, and  $A_d=6 \times 10^{-6}$  and  $B_d=-5 \times 10^{-6}$ . Normalized strain hardening exponent increases, but normalized fracture toughness decreases with increase of the degraded time. Hence normalized fracture toughness is a useful factor for evaluating the degree of material degradation.

Figure 7 shows the exponential relation between normalized fracture toughness and normalized Brinell hardness. That is,

$$\frac{K_Q}{K_{Q0}} = C_d - D_d e^{-F_d x} \quad (16)$$

where  $x = \frac{HB}{HB_0}$  and  $C_d=1.048$  and  $D_d=129.435$  and  $F_d=8.097$ . If normalized Brinell hardness can be obtained by BI test, normalized fracture toughness can be determined by Eq. (16) in case of 1Cr-1Mo-0.25V steels and it means that also the degree of material degradation can be determined by BI test.

The BI test is a quasi-nondestructive method to get material properties without the destruction of the material. This method has the strong points of being applicable to in-service facilities and being able to get reliable data without the influence of an experimentalist's skill and so on. It is expected to be able to estimate not only general mechanical properties like tensile strength and hardness but also fracture properties like fracture toughness and indentation energy to fracture at the viewpoint of material degradation.

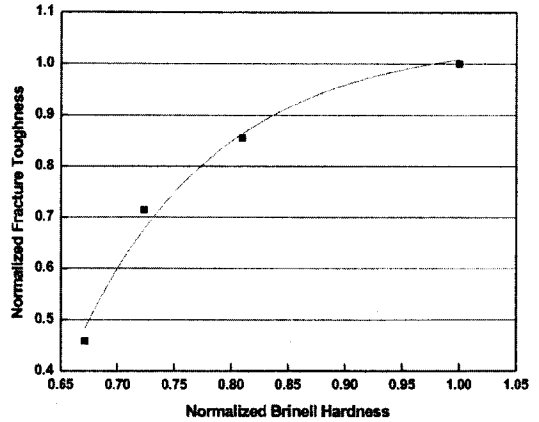


Fig. 7 Relation between normalized Brinell hardness and normalized fracture toughness at service temperature

## 5. Conclusions

In this study, the effect of aging in the degradation time range 0~1820 hours at constant aging temperature of 630°C on the mechanical behavior of 1Cr-1Mo-0.25V steels have been studied using the ball indentation system. The results are summarized as follows.

(1) Normalized Brinell hardness agrees well with others, i.e., tensile strength of BI tests, indentation energy to fracture(IEF) and tensile strength of tensile tests at the viewpoint of material degradation.

(2) Because fracture toughness is linearly related with in-service degraded time, normalized fracture toughness is a useful factor for evaluating the degree of material degradation.

(3) Because there is the exponential relation between normalized fracture toughness and normalized Brinell hardness of 1Cr-1Mo-0.25V steels, normalized fracture toughness can be determined by Brinell hardness.

## Acknowledgements

The authors are grateful for the support provided by a grant from Safety and Structural Integrity Research Centre at Sungkyunkwan University and the Brain Korea 21 Project in 2003.

## References

- Abdel-Latif, A. M., Corbett, S. M. and Taplin, D. M. R., 1982, *Metal Science*, Vol. 16, pp. 90~96.
- Haggag, F. M. and Murty, K. L., 1997, in: P. K. Liaw, O. Buck, R. J. Arsenault, R. E. Green Jr. (Eds.), *Non-destructive Evaluation and Materials Properties III*, TMS, Warrendale, PA, p. 101.
- Haggag, F. M. and Nanstad, R. K., 1989, "Estimating Fracture Toughness using Tension or Ball Indentation Tests and a Modified Critical Strain Model," *The American Society of Mechanical Engineers PVP*, Vol. 170, pp. 41~46.
- Haggag, F. M., et al., 1990, "Use of Automated Ball Indentation Testing to Measure Flow Properties and Estimate Fracture Toughness in Metallic Materials," *ASTM STP 1092*, pp. 188~208.
- Haggag, F. M., 1993, "In-Situ Measurements of Mechanical Properties Using Novel Automated Ball Indentation Systems," *Small Specimen Test Techniques Applied to Nuclear Reactor Vessel Thermal Annealing and Plant Life Extension*, *ASTM STP 1204*, pp. 27~44.
- Mathew, M. D. and Murty, K. L., 1999, "Non-destructive Studies on Tensile and Fracture Properties of Molybdenum at Low Temperatures," *Journal of Materials Science*, Vol. 33, pp. 1497~1503.
- Nham, S. H. and Kim, A. K., 1998, "Nondestructive Evaluation of Toughness Degradation of 1Cr-1Mo-0.25V Steel Using Electrical Resistivity," *Transaction of KSME A*, Vol. 22, No. 5, pp. 814~820.
- Seok, C. S., Kim, D. J. and Bae, B. K., 2000, "Evaluation of Material Degradation Using Electrical Resistivity Method," *Transaction of KSME A*, Vol. 24, No. 12, pp. 2992~3002.
- Tabor, D., 1951, *The Hardness of Metals*, Oxford University Press, New York.
- Yamashita, M., et al., 1997, "Service-induced Changes in the Microstructure and Mechanical Properties of a Cr-Mo-Ni-V Turbine Steel," *ISIJ International*, Vol. 37, No. 11, pp. 1133~1138.